THE JOURNAL OF PHYSICAL CHEMISTRY C

Article

pubs.acs.org/JPCC

Mechanism of Enhanced Carbon Cathode Performance by Nitrogen Doping in Lithium–Sulfur Battery: An X-ray Absorption Spectroscopic Study

Pengyu Zhu,[†] Jiangxuan Song,[‡] Dongping Lv,[‡] Donghai Wang,*[,‡] Cherno Jaye,[§] Daniel A. Fischer,[§] Tianpin Wu,[∥] and Yongsheng Chen*[,†]

[†]EMS Energy Institute, John and Willie Leone Family Department of Energy and Mineral Engineering, The Pennsylvania State University, University Park, Pennsylvania 16802, United States

[‡]Department of Mechanical & Nuclear Engineering, The Pennsylvania State University, University Park, Pennsylvania 16802, United States

[§]Material Measurement Laboratory, National Institute of Standards and Technology, Gaithersburg, Maryland 20899, United States

[∥]Advanced Photon Source, Argonne National Laboratory, Argonne, Illinois 60439, United States

Supporting Information

ABSTRACT: Lithium–sulfur batteries have drawn much attention in advanced energy storage development due to their high theoretical specific capacity; however, several obstacles hinder their applications, including rapid capacity loss due to dissolution of polysulfide into the electrolyte. Nitrogen-doped mesoporous carbon cathode materials were found to effectively immobilize sulfur species and minimize the sulfur loss. In this work, we use X-ray absorption near-edge structure (XANES) spectroscopy to probe the coordination structures of C, O, and N in a carbon cathode before and after the sulfur loading in order to better understand the effects of nitrogen doping. A significant change in oxygen coordination structure is observed, whereas the carbon and nitrogen chemical environments remain unaltered. In addition, the significant change in S K-edge XANES spectra is also observed after sulfur was loaded on nitrogen-doped carbon cathode material. These observations reveal that strong interaction between the nitrogen-doped carbon and sulfur is through oxygen functional groups, and nitrogen doping probably makes oxygen functional groups more reactive toward sulfur.

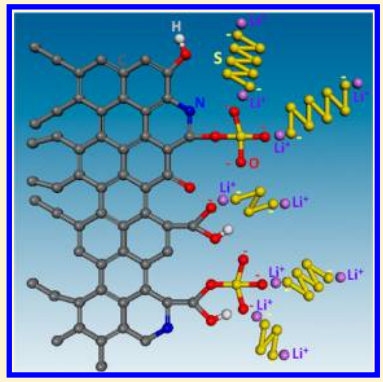

INTRODUCTION

Lithium–sulfur batteries are very attractive candidate for next-generation lithium battery systems due to its high theoretical specific capacity (1672 mAh g^{-1}) and energy density (2600 Wh kg^{-1}).[1] However, it is still far from commercialization mainly due to the low sulfur conductivity and low sulfur utilization caused by the shuttle effect.[2] Owing to the insulating nature of sulfur, conductive additives are needed to provide intimate contact in the cathode between sulfur and the immobilizer materials, such as carbon with a high surface area and large pore volume. Moreover, cleavage of sulfur–sulfur bonds occurs to the eight-atom sulfur (S_8) ring during the discharge process, and the resulting sulfur chain may undergo further cleavage and bond with lithium ions to form highly soluble polysulfide species Li_2S_n ($3 \leq n \leq 8$) in the organic electrolyte. As the discharge process proceeds further, eventually insoluble discharge products Li_2S_2 and Li_2S are formed. The production of highly soluble polysulfide intermediates in organic electrolyte causes loss of sulfur active materials via polysulfide dissolution and leads to fast capacity fading, low coulombic efficiency, and short cycle life of the sulfur electrode.[3−5] Many efforts have been devoted to overcoming these obstacles, e.g., introduction of additives such as $LiNO_3$ into the organic electrolyte, and developing of solid-state electrolyte, protective layers and novel sulfur–carbon cathodes.[5−10] In particular, the development of carbon–sulfur cathode materials has gained extensive attention owing to the highly conductive nature and readily designed porous structure of carbon-based materials that can improve the conductivity of a sulfur cathode and confine the soluble polysulfides in its pore structure.

Among various carbon materials, mesoporous carbon (pore size between 2 and 50 nm) has been mostly investigated. For the purpose of entrapping sulfur, tunable pore size and pore volume distributions have been achieved via different preparation methods. Li et al. synthesized mesoporous carbon–sulfur materials with various pore sizes (22, 12, 7, and 3 nm) and pore volumes (from 1.3 to 4.8 $cm^3\ g^{-1}$) as the framework for lithium–sulfur (Li–S) batteries.[11] Different sulfur loadings were studied, and the result indicated that, with a larger pore volume, the mesoporous carbon retained a higher

Received: December 17, 2013
Revised: February 19, 2014
Published: March 21, 2014

   dx.doi.org/10.1021/jp4123634 | J. Phys. Chem. C 2014, 118, 7765−7771

maximum sulfur loading. A sulfur content of 83 wt % was achieved for a 22 nm mesoporous carbon. However, the overall battery performance was very similar for different mesoporous carbon materials at full sulfur-filling conditions. Later, hierarchically structured carbon was introduced by Dudney et al., in which micropores (less than 2 nm) were introduced to the mesoporous carbon with a uniformly distributed 7.3 nm pore size.[12] In such a configuration, smaller pores yielded high surface area and were preferentially filled with sulfur, while bigger pores were able to confine the intermediate sulfur species and provide Li ionic pathways via facilitating electrolyte during the cycles.

Graphene has also become a research hotspot owing to its high conductivity and large surface area. Efforts have been taken to utilize the graphene structure as a host for sulfur species. In addition to the physical confinement and physical adsorption, chemical adsorption has been found to effectively entrap sulfur species. Oxygen functional groups on the graphene oxide (GO) anchored sulfur species to graphene sheets through chemical adsorption and resulted in the enhanced immobilization of later formed Li polysulfides.[13] Improved cycling stability and a reversible capacity of 950 mAh g^{-1} were reported.[14]

Nitrogen doping has already been employed to modify the properties of various carbon materials for broader applications. Usually, doping of a heteroatom, e.g., nitrogen or boron, alters the charge distribution of neighboring carbon atoms, which generates an activation region for catalytic reactions, e.g., oxygen reduction reaction (ORR) in fuel cells.[15,16] It was also reported that nitrogen doping created defects in the walls of carbon nanotubes (CNTs), serving as tunnels for Li ion transportation.[17] In addition, interactions between the nitrite and Li ions were used to enhance Li storage capability of the material that yielded high polysulfide retention.[18]

The widely accepted theory of nitrogen promotion was explained mainly by theoretical simulations[16] and electrochemical tests. Characterization techniques, such as BET, XRD, SEM, and TEM, were used to help understand the effects of nitrogen dopants. Coupled with electrochemical tests, enhanced performance can be correlated to an increase of surface area and good electrical and mechanical properties of materials.[17,19] X-ray photoelectron spectroscopy (XPS) was used to identify nitrogen species, and three main types were observed, namely, pyridinic, pyrrolic, and quaternary nitrogen.[20−22] Theoretical calculation was widely used to explain the enhancement of performance with nitrogen doping. For example, Gong et al. used quantum mechanics calculations and hybrid density functional theory to show that carbon atoms adjacent to nitrogen dopants possess a substantially higher positive charge due to the strong electronic affinity of the nitrogen atom.[15] Through DFT calculation, Zhang et al. concluded that the electron charge transfer between nitrogen and carbon provided active sites for ORR reaction.[16] Niwa et al. utilized X-ray absorption spectroscopy (XAS) to investigate the nitrogen species at the N K-edge in the cathode of polymer electrolyte fuel cells and found that graphite-like nitrogen exhibited a higher ORR activity than pyridine-like nitrogen.[23]

Inspired by the advantage of hierarchically structured carbon, we introduced nitrogen into a mesoporous carbon material and modified the oxygen functionalities on the carbon; as a result, better chemical adsorption was achieved for the sulfur immobilization.[24] A high capacity retention (~800 mAh g^{-1} after 100 cycle @ 0.1 C; 1 C = 1672 mAh g^{-1}) and high coulombic efficiency (~93%) were thus achieved. In this follow-up work, we utilize X-ray absorption near-edge structure (XANES) spectroscopy to probe the chemical environments around C, N, O, and S. With nitrogen doping, a significant change is found in the O coordination structure after sulfur loading. S K-edge XANES also confirms a direct significant change in the sulfur coordination structure. Thus, a mechanistic model of nitrogen-doping-promoted chemical adsorption of sulfur on the carbon material is proposed.

EXPERIMENTAL METHODS

Mesoporous carbon (MPC) and mesoporous nitrogen-doped carbon (MPNC) materials were prepared using poly(melamine-*co*-formaldehyde) resin (Sigma Aldrich, average molecular weight ~432, 84 wt % in 1-butanol) as a polymer precursor. Tetraethyl orthosilicate, amphiphilic triblock copolymer Pluronic F127 ($(EO)_{106}(PO)_{70}(EO)_{106}$) and colloidal silica (Nissan Chemical Industries, SNOWTEX-O, 10−20 nm) were used as porogens to obtain high pore volume and high surface area for sulfur loading and immobilizing purposes. Detailed preparation procedures were published in our previous work.[24] The MPNC−sulfur material was prepared by impregnating sulfur (Sigma Aldrich, 99.998% trace metals basis) in MPNC at 155 °C for 10 h with different sulfur loadings. When naming a sulfur-loaded sample, the sulfur content was denoted as a number following the S symbol, e.g., MPNC-S2 stands for an MPNC material loaded with 2 wt % sulfur. A MPNC-S70 cathode was used for Li−S battery performance evaluation. The cathode was prepared by mixing 80 wt % composite powder, 10 wt % Super P (commercial carbon black from Timcal Graphite & Carbon), and 10 wt % polyvinylidene fluoride (PVDF) together in *N*-methyl-2-pyrrolidinone (NMP) to form a slurry, which was then coated on an aluminum foil and dried at 60 °C for 10 h under vacuum. The electrochemical performance was tested in a half-cell configuration with MPNC-S70 as cathode and a lithium chip as anode in CR2016 type coin cells. The electrolyte was 1 M LiTFSI dissolved in a mixture of 1,3-dioxolane (DOL) and 1,2-dimethoxyethane (DME) (1:1 v/v), and the separator was a microporous polypropylene membrane (25 μm thick, Celgard 2400). Cells were assembled in an argon-filled glovebox, and the discharge/charge cycles were tested galvanostatically using a battery tester (Arbin BT-2000) at room temperature in a voltage window between 3 and 1.7 V.

For XANES experiments, MPC and MPNC materials were used as prepared in power forms, representing the chemical environment of the mesoporous carbon cathode. A maximum 5 wt % sulfur loading was applied to MPC and MPNC materials, representing the chemical environment of different cathode materials after the sulfur adsorption. All XANES spectra were collected ex-situ. C K-edge (284.2 eV), N K-edge (409.9 eV), and O K-edge (543.1 eV) XANES spectra were collected at the National Institute of Standards and Technology U7A Beamline at National Synchrotron Light Source (NSLS) at Brookhaven National Laboratory. The storage ring was operated with an electron beam energy of 800 MeV and an average current of 600 mA. The XANES spectra were collected in a partial electron yield mode with low-energy electron compensation to minimize the charging effect for poor conductors. Additionally, a clean gold-coated mesh was used to monitor I_o, the incident beam intensity. The data were processed using Athena.[25] Quantification of oxygen functional groups was performed with O K-edge spectra by a linear combination fitting method that was reported elsewhere.[26]

dx.doi.org/10.1021/jp4123634 | J. Phys. Chem. C 2014, 118, 7765−7771

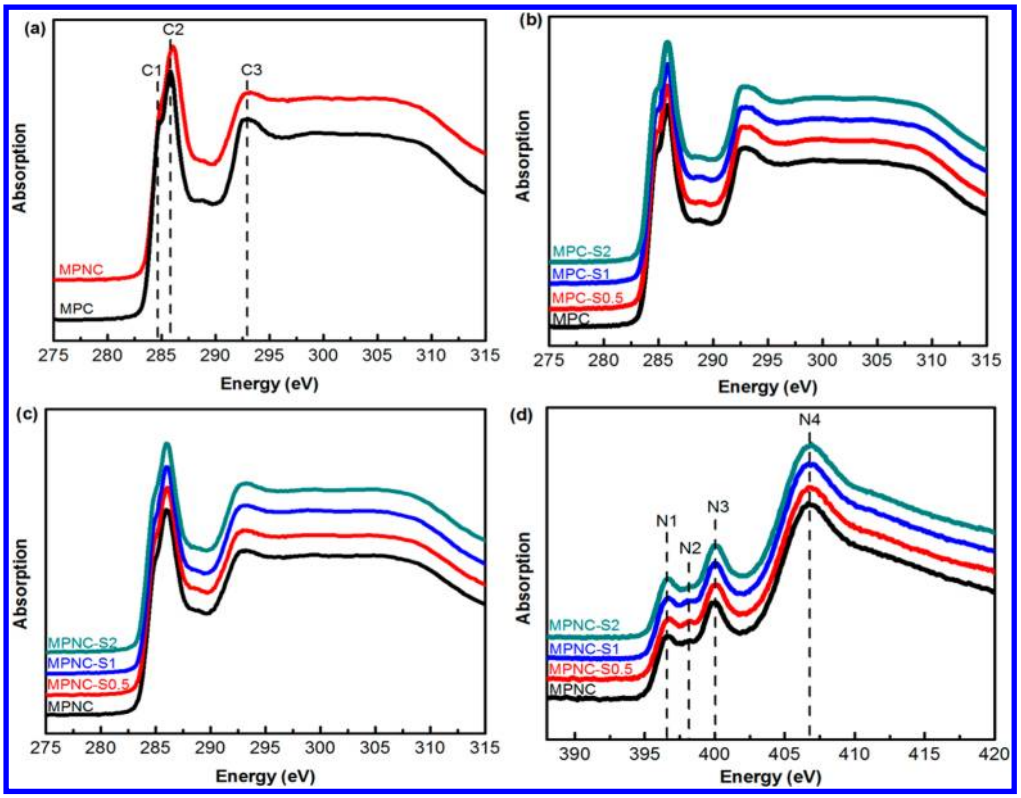

Figure 1. (a) C K-edge XANES of MPC and MPNC. (b) C K-edge XANES spectra of MPC with different sulfur loadings and (c) MPNC with different sulfur loadings. (d) N K-edge XANES spectra of MPNC composite with different sulfur loadings.

S K-edge (2472 eV) XANES spectra were collected at 9-BM Beamline of Advanced Photon Source (APS) at Argonne National Laboratory. A cryogenic double-crystal Si(111) monochromator was used along with a Rh-coated mirror to reduce harmonics. All spectra were collected in fluorescence yield mode with a Si DRIFT 4-element detector (Vortex) providing an energy resolution of approximately 0.3 eV at 2.5 keV. Helium purging in the incident light path and the sample chamber was utilized to minimize signal loss through air absorption. Energy calibration was accomplished by setting the edge energy of elemental sulfur to 2472.0 eV. The data were also processed using Athena.[25]

RESULTS AND DISCUSSION

The cycle discharge−charge performance test was conducted on MPNC-S80, MPC-S80, and C-S80 (Super P carbon black) cathodes in half-cell configurations. The initial discharge capacity of MPNC-S80 was 1013 mAh g^{-1} with a coulombic efficiency of over 90%. From the second cycle, a large reversible capacity of 1008 mAh g^{-1} was obtained, corresponding to a capacity retention of ∼99.5%. In contrast, MPC-S80 and C-S80 could only obtain a capacity retention at ∼86.6% and ∼91.1%, respectively. In addition, MPNC-S80 exhibited a high capacity retention of 80% and coulombic efficiency over 90% within 50 cycles at 0.17 mAh cm^{-2}, whereas MPC-S80 and C-80 cathodes showed faster capacity fading and much lower coulombic efficiency. Detailed electrochemical performance results can be found in our previous work.[24] The MPNC nanocomposite serves as an excellent immobilizer for sulfur and polysulfide species and minimizes the shuttle effect for retaining high coulombic efficiency during the discharge−charge process.

One interesting question is how the N doping modifies the performance of carbon−sulfur electrodes. Does it provide additional adsorption sites for polysulfide or does it affect the performance indirectly by causing changes in carbon surface functional groups? This question can be well-addressed by XANES since, when there is strong interaction through chemical adsorption, changes in coordination structure of the adsorption sites would occur, which can be readily captured by XANES.

The normalized C K-edge XANES spectra of MPC and MPNC materials without sulfur loadings are shown in Figure 1a. The main features include an absorption peak at 285.8 eV (C2) and a shoulder peak at 284.7 eV (C1), which are corresponding to the π^* resonance of aromatic carbon species (aromatic-C and quinone type-C, respectively).[27−29] The broad absorption band between 294 and 310 eV is a characteristic of graphite-like carbon materials. The σ^* band feature at ∼293 eV (C3) is the characteristic of the sp^3 tetrahedral C−C bond, which can serve as a good indicator of degree of graphitization.[30,31] Compared to MPNC materials, a higher intensity of the shoulder at 284.7 eV in MPC indicates the presence of more quinine type carbon. Clearly, the nitrogen dopant alters the chemical environment of carbon materials. In addition, the lower peak intensity at 293 eV in MPNC indicates a decrease of sp^3 tetrahedral C−C bonding, as a result of the C−C bond being replaced by graphitic C−N−C bonds.

Panels (b) and (c) in Figure 1 show the C K-edge XANES spectra of MPC and MPNC materials with different sulfur loadings, respectively. No changes in XANES spectra in MPC and MPNC are observed after sulfur loading, indicating no or negligible change in carbon coordination structure in MPC and MPNC after sulfur loading. The following reasons are proposed: (1) no formation of C−S bonds; (2) absorption features of C−S are similar to some other C species that C−S is replacing; or (3) the features of C−S are significantly different

dx.doi.org/10.1021/jp4123634 | J. Phys. Chem. C 2014, 118, 7765−7771

than other C species that are present, but the abundance of C−S is negligible since XANES is an average technique.

The N K-edge XANES were also collected on MPNC samples with different sulfur loadings to probe the nitrogen coordination structure. As shown in Figure 1d, four peaks are observed in the spectra, denoted as N1 through N4. Peaks N1 at 396.7 eV and N3 at 399.8 eV are attributed to the pyridinic (C═N π^*) and graphitic type nitrogen, respectively.[32] These results are in good accordance with C K-edge XANES spectra. The peak N2 at 398.2 eV, which is very weak, is assigned to the amino type species ($-NH_2$). The low peak intensity indicates very low abundance of amino type nitrogen in MPNC material. Peak N4 is not assigned to any nitrogen species; it is derived from the general transitions from the N 1s core level to C−N σ^* states.[32] With increasing loading of sulfur content, the N K-edge XANES spectra remain unchanged, which strongly suggests that sulfur does not directly interact with carbon through nitrogen bonding.

The O K-edge XANES spectra of MPC and MPNC materials were collected to probe the chemical environment of oxygen functional groups on the carbon materials before and after the sulfur loading and are shown in panels (a) and (b) in Figure 2,

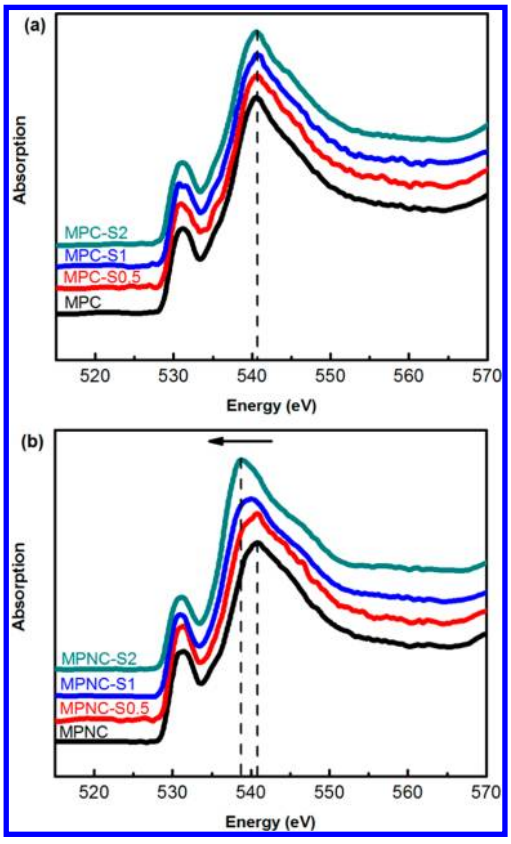

Figure 2. O K-edge XANES spectra of (a) MPC composite and (b) MPNC composite with different sulfur loadings.

respectively. As a general observation, O K-edge spectra consist of a pre-edge feature (sharp peak around 530 eV) and a broad white line (first intense post-edge peak, near 540 eV in this case). The pre-edge feature is attributed to the 1s→π^* transition in the C═O bond, while the broad white line is assigned to the 1s→σ^* transition in C−O bonds associated with various kinds of oxygen functional groups.[33] As shown in Figure 2, the pre-edge peak appears at 531.0 eV and the white line shows at 540.6 eV for MPC samples before and after sulfur loading. For the MPNC sample series, the pre-edge peaks remains at 531.1 eV, while the white line shifts from 540.9 to 538.8 eV with increasing sulfur loading.

The obvious white line shift of 2 eV strongly suggested a change of oxygen coordination structure when MPNC materials interact with sulfur, implying a direct chemical bonding between oxygen and sulfur. In contrast, without nitrogen doping, there is basically no change in oxygen functional groups on MPC materials with different sulfur loadings (Figure 2a). The results suggest that nitrogen doping affects the performance indirectly by making carbon surface functional groups more reactive toward sulfur.

To elucidate the change of oxygen chemical environment, more quantitative analysis of the oxygen functional groups is carried out. In our previous work, we established a method using O K-edge XANES spectroscopy to identify and quantify the oxygen-containing surface functional groups on active carbon materials.[26] Oxygen functional groups are grouped into three types, namely, carboxyl-type, carbonyl-type, and hydroxyl-type (ether-type), and their abundance is quantified by linear combination fitting (LCF). Here, we apply the method to the O K-edge spectra and quantify the oxygen functional groups on MPNC before and after sulfur loading. LCF was performed on O K-edge spectra on samples with the most contrast, namely, MPNC and MPNC-S2, with a fitting range from 10 eV before the edge to 25 eV beyond the edge, covering all pre-edge peaks and the characteristic white line region. All spectra, including the reference spectra used in the fitting,[26] were normalized to a unity edge step prior to the fitting. As shown in Figure 3, excellent fits are obtained for the two spectra, and the fitting result is presented in Table 1.

Evidently, a decrease in the abundance of carboxyl-type and carbonyl-type groups (from 54% to 40% and from 16% to 9%, respectively) is observed, whereas there is an increase of hydroxyl-type groups from 30% to 51% after sulfur loading. It appears that the C═O bond in both carboxyl-type and carbonyl-type groups are consumed to form hydroxyl-type groups, which include hydroxyls and esters. Formation of C−O−S would be hydroxyl-like in carbon XANES. The increase of hydroxyl-type groups and decrease of carboxyl-type and carbonyl-type groups on the MPNC-S2 sample strongly suggest the formation of C−O−S bonds. Nitrogen seems to play an important role in the process. With a higher electronegativity of nitrogen than carbon, the electron density on the C═O bond adjacent to a nitrogen dopant is altered and the bond strength is weakened, which makes it more reactive. As a result, MPNC material can better immobilize sulfur species through C−O−S bridges. For MPC samples, no obvious change in oxygen chemical environment is found, suggesting no strong chemical bonding between MPC composites and sulfur.

Sulfur has multiple valence states, and different sulfur species have characteristic absorption peaks in S K-edge XANES spectra, so in turn, the sulfur oxidation states can be determined by its absorption peaks. The elemental sulfur has an absorption edge energy of 2472 eV and a strong absorption peak at 2472.8 eV and a broad band at 2479.7 eV. The sulfate species with a +6 valence state possesses one single peak at 2482.5 eV. Sulfur oxidation states can be readily distinguished in K-edge XANES spectra due to the wide energy shift (1.5−1.6 eV) associated with each unit change of S oxidation state. Thiosulfate shows two major characteristic peaks at 2472 and 2481.2 eV, associated with −1 and +5 valence sulfur atoms.[34,35] In

dx.doi.org/10.1021/jp4123634 | J. Phys. Chem. C 2014, 118, 7765−7771

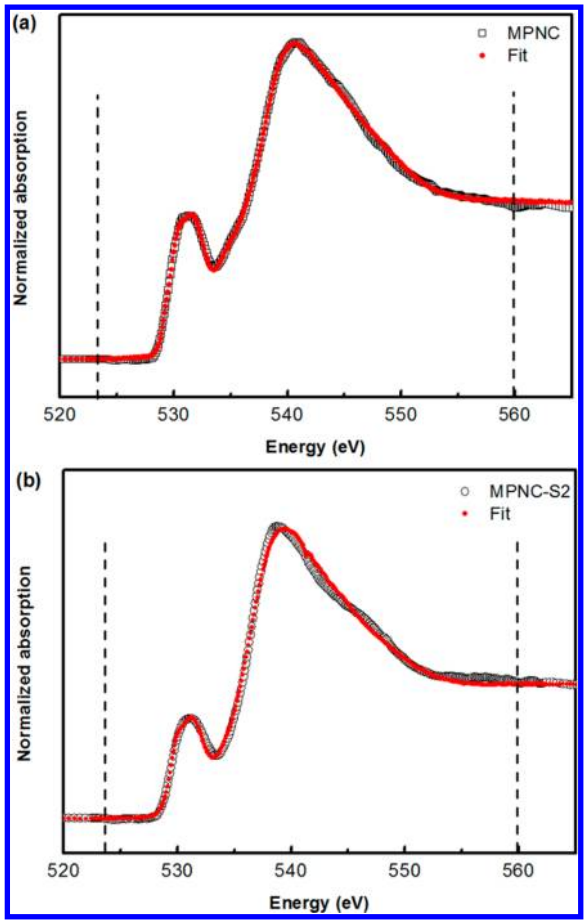

Figure 3. Linear combination fitting of O K-edge XANES spectra of (a) MPNC and (b) MPNC-S2 with fitting range shown. Both spectra are normalized to a unit edge height.

Table 1. Abundance of Different Types of Oxygen Functional Groups in MPNC and MPNC-S2

	MPNC	MPNC-S2
carbonyl-type groups[a]	16%	9%
carboxyl-type groups[b]	54%	40%
hydroxyl-type groups[c]	30%	51%
R-factor	0.00013	0.00085

[a]Includes carbonyl, aldehyde, and ketone. [b]Includes carboxylic acid, anhydride, and ester. [c]Includes phenolic hydroxyl, aliphatic hydroxyl, and ether.

addition, a shoulder appears at 2479.2 eV, which is attributed to the electronic transition from 1s to antibonding orbital a1* of the +5 valence S atom.[36] Similarly, in the tetrathionate XANES spectrum, a characteristic peak of +5 valence S at 2482.1 eV and another peak at 2478.3 eV are observed.[34]

Cuisinier et al. recently reported sulfur speciation in Li−S batteries using in situ XANES spectroscopy, revealing the sulfur redox chemistry during cycling.[37] Elemental sulfur, polysulfide species, and Li_2S were observed by S K-edge XANES in operando condition. The evolution of sulfur species in the electrochemical cycling was interpreted by liner combination fitting of reference spectra, including α-S_8, S_6^{2-}, S_4^{2-}, S_2^{2-}, and Li_2S. In this study, we focus on the interaction between sulfur and the carbon cathode and utilize S K-edge XANES to probe chemical bonding between sulfur and the functional groups present on the carbon surface. To optimize the sensitivity to the interaction between the carbon cathode and sulfur, a low content of sulfur loading (maximum 5 wt %) was used, a condition that is different than that in an operating battery. The XANES spectra of MPC and MPNC with different sulfur loadings are recorded ex situ and are shown in Figure 4.

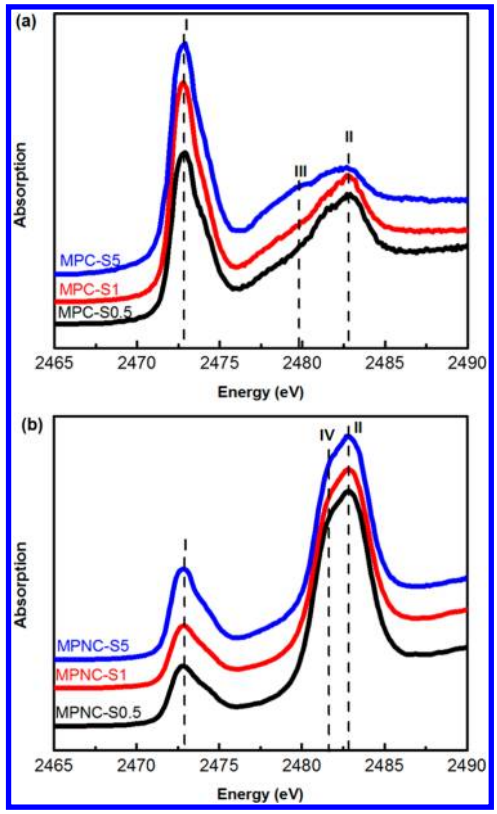

Figure 4. (a) S K-edge XANES spectra of MPC-S0.5, MPC-S1, and MPC-S2. (b) S K-edge XANES spectra of MPNC-S0.5, MPNC-S1, and MPNC-S2.

Two major peaks are observed in both MPC and MPNC series, peak I at 2472.8 eV and peak II at 2482.8 eV. In the MPC series, peak I and the flat broad peak III at 2479.7 eV are coincident with those of the elemental sulfur. However, peak III of the elemental sulfur is almost invisible due to superimposition of peak II at 2482.8 eV, which is a sulfate species in the system resulting from the interaction between the carbon material and the sulfur that was loaded. In the MPNC series, a huge increase in intensity of peak II is observed, indicating a drastic increasing of the sulfate species in the system when the carbon substrate is doped with nitrogen.[38] In addition, a small shoulder peak at 2481.7 eV is discernible, which suggests the presence of a minor thiosulfate species. The other thiosulfate absorption peak at 2472 eV is very close to the main absorption peak of elemental sulfur, and thus not obvious. The sulfur XANES results show that the interaction between elemental sulfur (S8) and nitrogen-doped carbon produces more sulfate (and possible thiosulfate) species than the carbon without nitrogen doping. Now the question becomes how sulfate (and thiosulfate) species may improve sulfur retaining in the carbon cathode.

Recall the previous XANES results of the carbon substrate that, after sulfur loading, only the oxygen coordination structure undergoes significant change. We propose that the sulfate (and thiosulfate) species that were observed in XANES are carbon

dx.doi.org/10.1021/jp4123634 | J. Phys. Chem. C 2014, 118, 7765−7771

Scheme 1. Possible Sulfur-Containing Functional Groups on MPNC Materials

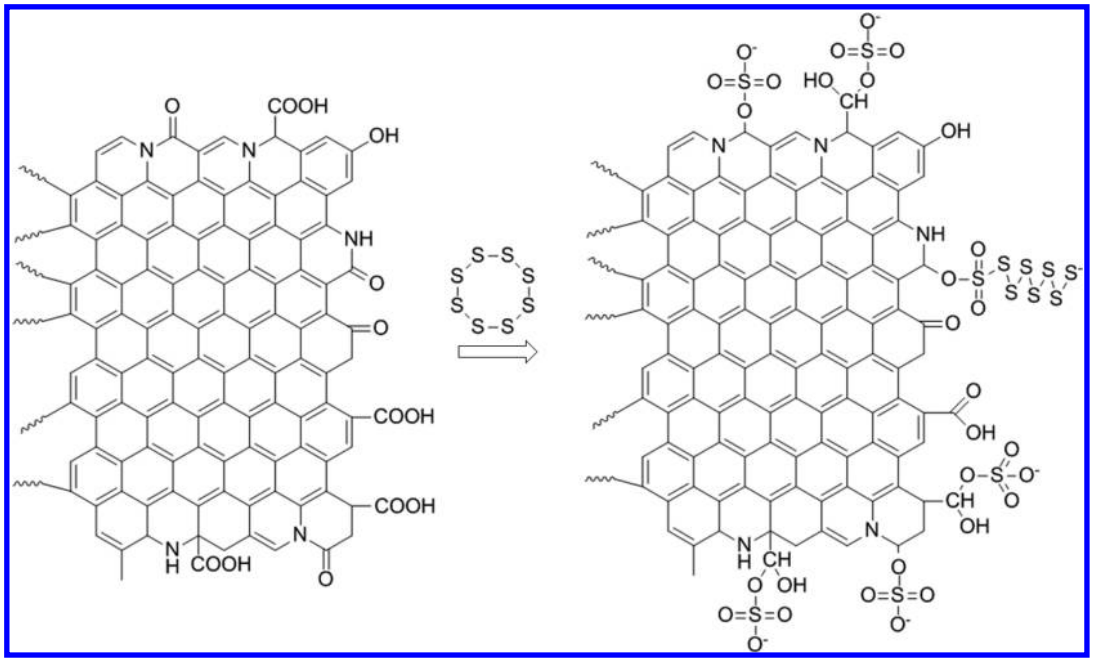

surface functional groups, as shown in Scheme 1. These sulfur species are fixed on the carbon substrate by sharing an oxygen and act as adsorption sites for other sulfur species that participate in electrochemical processes. The oxygen ions on the carbon substrate are charge centers, which provide anchoring sites for Li^+ ions through attractive electrostatic interaction. Generation of tethered surface sulfate species on the carbon substrate by consuming one oxygen site while adding three more oxygen sites effectively increases anchoring sites for Li^+ ions. During charge/discharge processes, adsorbed Li^+ ions become strong adsorption sites for various lengths of negatively charged sulfur chains. These sulfur chains end with other Li^+ ions and may abstract more sulfur chains. In addition, the long sulfur chain connected to the possible thiosulfate structure will interact strongly with the long sulfur chain that results from the initial sulfur ring (S8) opening. Thus, sulfur retaining is improved.

CONCLUSIONS

Nitrogen-doped mesoporous carbon cathode materials exhibited much better sulfur immobilization capability than their undoped counterpart. We have utilized XANES to elucidate the mechanism of enhanced cathode performance by probing the chemical environment of C, N, O, and/or S in MPC and MPNC cathode materials before and after sulfur loading. The N K-edge XANES showed no change in the N coordination structure after sulfur loading, suggesting that nitrogen does not directly form chemical bonds with sulfur for the sulfur immobilization. In other words, nitrogen does not provide extra active sites for sulfur adsorption. Meanwhile, a transformation of oxygen functional groups was observed in O K-edge XANES spectra when MPNC materials adsorbed sulfur species, whereas MPC materials without nitrogen doping did not show such a trend. In addition, S K-edge XANES showed that the interaction between elemental sulfur (S8) and nitrogen-doped carbon produces more thiosulfate and sulfate species than the carbon without nitrogen doping. Thus, we conclude that, with the presence of nitrogen, the surface oxygen functional groups become more reactive, and the formation of thiosulfate and sulfate species fixed on the carbon cathode is more significant. These sulfur-containing functional groups provide excellent adsorption sites for sulfur species that are generated in the electrochemical processes pertaining to battery operation.

ASSOCIATED CONTENT

Supporting Information

Infrared spectra of MPNC materials before and after sulfur loading. This material is available free of charge via the Internet at http://pubs.acs.org.

AUTHOR INFORMATION

Corresponding Authors

*Phone: +1-814-863-1287. E-mail: dwang@psu.edu (D.W.).
*Phone: +1-814-865-9834. E-mail: yzc2@psu.edu (Y.C.).

Notes

Disclaimer. Certain commercial names are mentioned in this article only for the purpose of illustration and do not represent an endorsement by the National Institute of Standards and Technology.

The authors declare no competing financial interest.

ACKNOWLEDGMENTS

XANES experiments conducted on U7A Beamline at the National Synchrotron Light Source (Brookhaven National Laboratory) were supported by the U.S. Department of Energy, Office of Basic Energy Sciences, under Contract DE-AC02-98CH10886. Use of the Advanced Photon Source, an Office of Science User Facility operated for the U.S. Department of Energy (DOE), Office of Science, by Argonne National Laboratory, was supported by the U.S. DOE under Contract No. DE-AC02-06CH11357.

REFERENCES

(1) Bruce, P. G.; Scrosati, B.; Tarascon, J.-M. Nanomaterials for Rechargeable Lithium Batteries. *Angew. Chem., Int. Ed.* **2008**, *47*, 2930−2946.

(2) Manthiram, A.; Fu, Y.; Su, Y. S. Challenges and Prospects of Lithium−Sulfur Batteries. *Acc. Chem. Res.* **2013**, *46*, 1125−1134.

(3) Kolosnitsyn, V. S.; Karaseva, E. V. Lithium-Sulfur Batteries: Problems and Solutions. *Russ. J. Electrochem.* **2008**, *44*, 506−509.

(4) Mikhaylik, Y. V.; Akridge, J. R. Polysulfide Shuttle Study in the Li/S Battery System. *J. Electrochem. Soc.* **2004**, *151*, A1969−A1976.

(5) Ji, X.; Evers, S.; Black, R.; Nazar, L. F. Stabilizing Lithium−Sulphur Cathodes Using Polysulphide Reservoirs. *Nat. Commun.* **2011**, *2*, 325.

(6) Ji, X.; Lee, K. T.; Nazar, L. F. A Highly Ordered Nanostructured Carbon−Sulphur Cathode for Lithium−Sulphur Batteries. *Nat. Mater.* **2009**, *8*, 500−506.

(7) Aurbach, D.; Pollak, E.; Elazari, R.; Salitra, G.; Kelley, C. S.; Affinito, J. On the Surface Chemical Aspects of Very High Energy Density, Rechargeable Li−Sulfur Batteries. *J. Electrochem. Soc.* **2009**, *156*, A694−A702.

(8) Hassoun, J.; Scrosati, B. Moving to a Solid-State Configuration: A Valid Approach to Making Lithium-Sulfur Batteries Viable for Practical Applications. *Adv. Mater.* **2010**, *22*, 5198−5201.

(9) Su, Y.-S.; Manthiram, A. A New Approach to Improve Cycle Performance of Rechargeable Lithium−Sulfur Batteries by Inserting a Free-Standing MWCNT Interlayer. *Chem. Commun.* **2012**, *48*, 8817−8819.

(10) Su, Y.-S.; Manthiram, A. Lithium−Sulphur Batteries with a Microporous Carbon Paper as a Bifunctional Interlayer. *Nat. Commun.* **2012**, *3*, 1166.

(11) Li, X.; Cao, Y.; Qi, W.; Saraf, L. V.; Xiao, J.; Nie, Z.; Mietek, J.; Zhang, J.-G.; Schwenzer, B.; Liu, J. Optimization of Mesoporous Carbon Structures for Lithium−Sulfur Battery Applications. *J. Mater. Chem.* **2011**, *21*, 16603−16610.

(12) Liang, C.; Dudney, N. J.; Howe, J. Y. Hierarchically Structured Sulfur/Carbon Nanocomposite Material for High-Energy Lithium Battery. *Chem. Mater.* **2009**, *21*, 4724−4730.

(13) Li, N.; Zheng, M.; Lu, H.; Hu, Z.; Shen, C.; Chang, X.; Ji, G.; Cao, J.; Shi, Y. High-Rate Lithium−Sulfur Batteries Promoted by Reduced Graphene Oxide Coating. *Chem. Commun.* **2012**, *48*, 4106−4108.

(14) Ji, L.; Rao, M.; Zheng, H.; Zhang, L.; Li, Y.; Duan, W.; Guo, J.; Cairns, E. J.; Zhang, Y. Graphene Oxide as a Sulfur Immobilizer in High Performance Lithium/Sulfur Cells. *J. Am. Chem. Soc.* **2011**, *133*, 18522−18525.

(15) Gong, K.; Du, F.; Xia, Z.; Durstock, M.; Dai, L. Nitrogen-Doped Carbon Nanotube Arrays with High Electrocatalytic Activity for Oxygen Reduction. *Science* **2009**, *323*, 760−764.

(16) Zhang, L.; Xia, Z. Mechanisms of Oxygen Reduction Reaction on Nitrogen-Doped Graphene for Fuel Cells. *J. Phys. Chem. C* **2011**, *115*, 11170−11176.

(17) Shin, W. H.; Jeong, H. M.; Kim, B. G.; Kang, J. K.; Choi, J. W. Nitrogen-Doped Multiwall Carbon Nanotubes for Lithium Storage with Extremely High Capacity. *Nano Lett.* **2012**, *12*, 2283−2288.

(18) Guo, J.; Yang, Z.; Yu, Y.; Abruña, H. D.; Archer, L. A. Lithium−Sulfur Battery Cathode Enabled by Lithium−Nitrile Interaction. *J. Am. Chem. Soc.* **2012**, *135*, 763−767.

(19) Maldonado, S.; Stevenson, K. J. Influence of Nitrogen Doping on Oxygen Reduction Electrocatalysis at Carbon Nanofiber Electrodes. *J. Phys. Chem. B* **2005**, *109*, 4707−4716.

(20) Wang, H.; Maiyalagan, T.; Wang, X. Review on Recent Progress in Nitrogen-Doped Graphene: Synthesis, Characterization, and Its Potential Applications. *ACS Catal.* **2012**, *2*, 781−794.

(21) Qie, L.; Chen, W. M.; Wang, Z. H.; Shao, Q. G.; Li, X.; Yuan, L. X.; Hu, X. L.; Zhang, W. X.; Huang, Y. H. Nitrogen-Doped Porous Carbon Nanofiber Webs as Anodes for Lithium Ion Batteries with a Superhigh Capacity and Rate Capability. *Adv. Mater.* **2012**, *24*, 2047−2050.

(22) Yang, S.; Feng, X.; Wang, X.; Mullen, K. Graphene-Based Carbon Nitride Nanosheets as Efficient Metal-Free Electrocatalysts for Oxygen Reduction Reactions. *Angew. Chem., Int. Ed.* **2011**, *50*, 5339−5343.

(23) Niwa, H.; Horiba, K.; Harada, Y.; Oshima, M.; Ikeda, T.; Terakura, K.; Ozaki, J.-i.; Miyata, S. X-ray Absorption Analysis of Nitrogen Contribution to Oxygen Reduction Reaction in Carbon Alloy Cathode Catalysts for Polymer Electrolyte Fuel Cells. *J. Power Sources* **2009**, *187*, 93−97.

(24) Song, J.; Xu, T.; Gordin, M. L.; Zhu, P.; Lv, D.; Jiang, Y. B.; Chen, Y.; Wang, D. Nitrogen-Doped Mesoporous Carbon Promoted Chemical Adsorption of Sulfur and Fabrication of High-Areal-Capacity Sulfur Cathode with Exceptional Cycling Stability for Lithium-Sulfur Batteries. *Adv. Funct. Mater.* **2014**, *24*, 1243−1250.

(25) Ravel, B.; Newville, M. ATHENA, ARTEMIS, HEPHAESTUS: Data Analysis for X-ray Absorption Spectroscopy Using IFEFFIT. *J. Synchrotron Radiat.* **2005**, *12*, 537−541.

(26) Kim, K.; Zhu, P.; Li, N.; Ma, X.; Chen, Y. Characterization of Oxygen Containing Functional Groups on Carbon Materials with Oxygen K-Edge X-ray Absorption Near Edge Structure Spectroscopy. *Carbon* **2011**, *49*, 1745−1751.

(27) Solomon, D.; Lehmann, J.; Kinyangi, J.; Liang, B.; Schäfer, T. Carbon K-Edge NEXAFS and FTIR-ATR Spectroscopic Investigation of Organic Carbon Speciation in Soils. *Soil Sci. Soc. Am. J.* **2005**, *69*, 107−119.

(28) Nikitin, A.; Ogasawara, H.; Mann, D.; Denecke, R.; Zhang, Z.; Dai, H.; Cho, K.; Nilsson, A. Hydrogenation of Single-Walled Carbon Nanotubes. *Phys. Rev. Lett.* **2005**, *95*, 225507.

(29) Xie, C.; Chen, Y.; Li, Y.; Wang, X.; Song, C. Influence of Sulfur on the Carbon Deposition in Steam Reforming of Liquid Hydrocarbons over CeO_2−Al_2O_3 Supported Ni and Rh Catalysts. *Appl. Catal., A* **2011**, *394*, 32−40.

(30) Kikuma, J.; Tonner, B. P. XANES Spectra of a Variety of Widely Used Organic Polymers at the C K-Edge. *J. Electron Spectrosc. Relat. Phenom.* **1996**, *82*, 53−60.

(31) Ray, S. C.; Pao, C. W.; Tsai, H. M.; Bose, B.; Chiou, J. W.; Pong, W. F.; DasGupta, D. Orientation of Graphitic Planes during Annealing of "Dip Deposited" Amorphous Carbon Film: A Carbon K-Edge X-ray Absorption Near-Edge Study. *Carbon* **2006**, *44*, 1982−1985.

(32) Zhang, L.-S.; Liang, X.-Q.; Song, W.-G.; Wu, Z.-Y. Identification of the Nitrogen Species on N-Doped Graphene Layers and Pt/NG Composite Catalyst for Direct Methanol Fuel Cell. *Phys. Chem. Chem. Phys.* **2010**, *12*, 12055−12059.

(33) Jeong, H. K.; Noh, H. J.; Kim, J. Y.; Jin, M. H.; Park, C. Y.; Lee, Y. H. X-ray Absorption Spectroscopy of Graphite Oxide. *Europhys. Lett.* **2008**, *82*, 67004.

(34) Morra, M. J.; Fendorf, S. E.; Brown, P. D. Speciation of Sulfur in Humic and Fulvic Acids Using X-ray Absorption Near-Edge Structure (XANES) Spectroscopy. *Geochim. Cosmochim. Acta* **1997**, *61*, 683−688.

(35) McKeown, D. A.; Muller, I. S.; Gan, H.; Pegg, I. L.; Stolte, W. C. Determination of sulfur Environments in Borosilicate Waste Glasses Using X-ray Absorption Near-Edge Spectroscopy. *J. Non-Cryst. Solids* **2004**, *333*, 74−84.

(36) Vairavamurthy, A.; Manowitz, B.; Luther Iii, G. W.; Jeon, Y. Oxidation State of Sulfur in Thiosulfate and Implications for Anaerobic Energy Metabolism. *Geochim. Cosmochim. Acta* **1993**, *57*, 1619−1623.

(37) Cuisinier, M.; Cabelguen, P.-E.; Evers, S.; He, G.; Kolbeck, M.; Garsuch, A.; Bolin, T.; Balasubramanian, M.; Nazar, L. F. Sulfur Speciation in Li−S Batteries Determined by Operando X-ray Absorption Spectroscopy. *J. Phys. Chem. Lett.* **2013**, *4*, 3227−3232.

(38) Solomon, D.; Lehmann, J.; Martínez, C. E. Sulfur K-Edge XANES Spectroscopy as a Tool for Understanding Sulfur Dynamics in Soil Organic Matter. *Soil Sci. Soc. Am. J.* **2003**, *67*, 1721−1731.